Available online at www.sciencedirect.com
ScienceDirect
Catalysis Today 118 (2006) 402–409
CATALYSIS TODAY
www.elsevier.com/locate/cattod

Cumene hydrocracking and thiophene HDS on niobia-supported Ni, Mo and Ni–Mo catalysts

Arnaldo C. Faro Jr.[a,*], Ana Carlota B. dos Santos [b]

[a] *Departamento de Físico-Química, Instituto de Química, UFRJ, Ilha do Fundão, CT, bloco A, CEP: 21949-900, Rio de Janeiro, RJ, Brazil*
[b] *PETROBRAS/CENPES/HTPE, Ilha do Fundão, Q. 7, CEP: 21949-900, Rio de Janeiro, RJ, Brazil*

Available online 1 September 2006

Abstract

Results are reported on the XPS characterization and catalytic activity in cumene hydrocracking (2.8 MPa, 623 K) and thiophene HDS (2.8 MPa, 523–573 K) of sulfided Ni, Mo and Ni–Mo catalysts supported on alumina and on pure and phosphated niobia. From the XPS results, evidence was obtained for the formation of a surface niobium sulfide with stoichiometry close to NbS_2 during catalyst sulfidation. Sintering of supported nickel during sulfidation occurred to a much smaller extent with the niobia-supported catalysts than with the alumina-supported ones. The dispersion of alumina-supported molybdenum was little influenced by sulfidation, whereas, with the niobia supports, the molybdenum surface concentration increased with sulfidation. With the alumina support, the Ni–Mo combination caused the dispersion of the sulfided nickel to be improved, possibly due to formation of a NiMoS phase. This was not observed with the niobia-supported catalysts.

Reasonable linear correlations were also found between the intrinsic activity for cumene hydrocracking and the amount of sulfided niobium in the catalysts, but the catalysts supported on phosphated niobia had a higher intrinsic activity than the ones supported on pure niobia. In thiophene HDS, the activity of the niobia-supported nickel catalysts was much larger than the activity of the alumina-supported ones. The activity of the niobia-supported molybdenum catalysts was smaller than that of the alumina-supported catalyst. With the bimetallic catalysts, little or no synergy was observed with the niobia-supported catalysts, in sharp contrast with the alumina case.

Keywords: Thiophene HDS; Cumene hydrocracking; Support effect; Niobium oxide; XPS; Ni–Mo catalysts

1. Introduction

Hydroprocessing of petroleum feeds includes hydrotreating (HDT) and hydrocracking (HCC) processes. The former are aimed at removing undesirable contaminants from petroleum feeds, such as sulfur, nitrogen and aromatic compounds, by reaction with hydrogen, while the latter are aimed at producing valuable light and medium distillates, such as naphtha, kerosene and diesel fractions, from heavy distillates and residues, also by reaction in the presence of hydrogen.

The increasing stringency of environmental laws and the need to process increasingly heavy feeds have stimulated the need to develop more efficient hydroprocessing catalysts. More specifically, environmental legislation throughout the world points towards maximum sulfur levels in fuels in the ppm level, and properties that were not formerly specified, such as diesel cetane number and the content of aromatic hydrocarbons in diesel and naphtha, are now subjected to legal limitation [1,2].

For many decades, industrial hydroprocessing catalysts have been comprised of bimetallic transition metal sulfides (Co–Mo, Ni–Mo and Ni–W), generally supported on γ-alumina. In HDT catalysts, silica or phosphate promoters are frequently used and, in HCC catalysts, an acidic component, such as fluoride or a zeolite, is normally added or, alternatively, an acidic support is used instead of alumina, such as amorphous silica-alumina (ASA).

The investigation of new hydroprocessing catalysts may involve research on new active phases, new promoters or new supports. The present paper is related to the third of these categories.

Alumina presents many advantages over other support materials. It is a low cost material, its surface area and pore size distribution are easy to control and it has good mechanical

* Corresponding author. Tel.: +55 21 590 9890; fax: +55 21 290 4746.
E-mail addresses: farojr@iq.ufrj.br (A.C. Faro Jr.), carlota@petrobras.com.br (A.C.B. dos Santos).

0920-5861/$ – see front matter
doi:10.1016/j.cattod.2006.07.027

strength and thermal stability. However, it also presents some drawbacks for application as a support for hydroprocessing catalysts, such as a strong interaction with molybdenum and nickel oxides, which may lead to incomplete conversion to sulfides during usual industrial sulfidation conditions, and a modest acidity, which is important for HCC reactions. Encouraging results have been obtained with other oxides, such as titanium [3,4] and zirconium oxides [5,6] or mixed oxides containing these elements [7], in terms of activity per molybdenum atom in the catalysts. This improvement is attributed to effects such as increase in dispersion of the active phases, more adequate active phase–support interaction, acidity effects and geometrical effects resulting in greater exposure of the active sites [8].

There are few reports in the literature on the use of a related transition metal oxide, namely niobium oxide, as a support for hydroprocessing catalysts. Yet, the few existing ones suggest that it is a promising material for this purpose, especially when an acidic function is desired. It is well known that niobium compounds, such as the oxide [9], phosphate [10] and sulfides (NbS_2 and NbS_3) [11] have acidic properties. Niobium oxide may be sulfided under appropriate conditions [12] and the niobium sulfides are active in HCC [13,14], hydrodenitrogenation (HDN) [13,14] and hydrodesulfurization (HDS) reactions [12,15]. Niobium-doped alumina-supported Ni–Mo catalysts have been found more active in cumene HCC and pyridine HDN than the undoped catalyst or the ones doped with boron, magnesium, titanium or zinc [16]. Weissman showed that Ni–Mo catalysts supported on surface and bulk niobium-aluminum oxides had higher activity in gasoil HDS and HDN than the pure supports [17].

A Ni–W catalyst supported on phosphate-additivated niobia was the only one to have a high and sustained activity in cumene HCC, as compared to others supported on sulfate-additivated Nb_2O_5, TiO_2, SnO_2, ZrO_2 and ZrO_2–SnO_2 [18].

From XPS measurements, we showed that a surface niobium species with a stoichiometry close to NbS_2 is formed when niobia-supported nickel or molybdenum catalysts are sulfided in a H_2S/H_2 mixture at 673 K. A linear correlation was found between activity in cumene HCC at 623 K and the amount of the sulfided niobium species. The presence of phosphate in the catalysts led to inhibition of the reduction–sulfidation of the support [19].

More recently we reported results on the characterization of the oxide form of niobia-supported Ni, Mo and Ni–Mo catalysts, comparatively to the alumina-supported materials [20]. It was found that on niobia there is a strong molybdena–support interaction, possibly with formation of a mixed niobium-molybdenum oxide, in contrast with the alumina case, where the molybdenum is present in a highly dispersed state as polymolybdate species. The alumina support strongly stabilizes supported oxidic nickel species towards reduction, in contrast with the niobia support. On alumina, the nickel and the molybdenum oxidic species, when simultaneously present in the catalysts, interact preferentially with each other rather than with the support, whereas the opposite is true of the niobia support.

In this paper we extend the results of our previous publication on XPS characterization and cumene HCC activity of niobia-supported hydroprocessing catalysts in the sulfided state [19] by including the bimetallic Ni–Mo series of catalysts and we report on their activity in the thiophene hydrogenolysis reaction, commonly used as a model reaction for HDS. Results are also included on the effect on catalytic activity of phosphorus addition to the niobia support.

2. Experimental

2.1. Catalyst preparation

The niobia support was obtained by calcination for 3 h at 723 K of a niobic acid sample ($Nb_2O_5 \cdot xH_2O$, 20.3% loss on ignition at 1073 K) furnished by Companhia Brasileira de Metalurgia e Mineração—CBMM. This support will be referred to as NB. A phosphorus-additivated niobia support was obtained by adsorption from a 1 mol dm^{-3} aqueous phosphoric acid solution, followed by filtration, drying at 393 K and calcination for 3 h at 723 K. This support will be referred to as NBP. The same calcination procedure was used for obtaining the alumina support, using as starting material a high purity commercial boehmite made by CONDEA Chemie (Pural SB, 24.0% loss on ignition at 1073 K). This support will be referred to as AL.

The catalysts were prepared by incipient wetness impregnation of the supports with aqueous solutions of the precursor salts: nickel nitrate—$Ni(NO_3)_2 \cdot 6H_2O$ and ammonium heptamolybdate—$(NH_4)_6Mo_7O_{24} \cdot 4H_2O$.

For the molybdenum impregnation, the heptamolybdate was dissolved in a 21 vol.% aqueous solution of hydrogen peroxide and the pH of the final solutions was adjusted to a value of 2 by nitric acid addition. For the nickel impregnations, the solutions were used at their natural pH values of ca. 3.7. Each impregnation was followed by drying at 393 K for 1 h and calcination in a static-air furnace at 723 K for 3 h.

The Ni–Mo catalysts were prepared by impregnation of the molybdenum catalysts with nickel solutions, as described above.

Nominal metal loadings, on an atom per support area basis, were kept the same for corresponding catalysts in the AL, NB and NBP series of catalysts. Thus, the molybdenum loading was 4.6 atoms nm^{-2} in all catalysts containing this element. In the nickel catalysts, loadings of 1.6, 3.7 and 5.5 atoms nm^{-2} were used. With the Ni–Mo catalysts, the Ni/Mo atomic ratios were 0.4, 0.8 and 1.2. The nickel loadings in the bimetallic catalysts were approximately the same as in the monometallic nickel catalysts.

The molybdenum catalysts will be referred to by the symbol corresponding to the support, followed by letter M. With the nickel catalysts, the symbol M is replaced by letter N and followed by a number from 1 to 3, which increases with the nickel content. An analogous scheme was used for the Ni–Mo catalyst, except that symbol N is replaced by NM. Thus, for example, the designation NB-NM1 refers to the niobia-supported nickel–molybdenum catalyst with the lowest nickel content.

2.2. Characterization

2.2.1. Surface areas

Surface areas of the supports and catalysts were determined by nitrogen adsorption at its normal boiling point using the

one-point BET method at a relative pressure of 0.3. The measurements were performed in a Micromeritics 2200 apparatus and the samples were dried in situ at 523 K before each measurement.

2.2.2. XPS measurements

The XPS measurements were performed in a Surface Science SSI instrument with monochromatized Al Kα (1486.6 eV) X-ray source. Charging effects were minimised by means of a flood gun adjusted to 8 eV. Binding energies corresponding to O 1s, Al 2p, Nb 3d, Mo 3d and Ni 2p electrons were referenced to the C 1s line, taken as 284.8 eV. Spectral intensities were measured in terms of the peak areas and converted to atomic percentage of each element, assuming a homogeneous distribution of the elements in the samples, using Scofield cross-sections.

Sulfided catalysts were analysed after sulfidation under flow of a 15 mol% H_2S in H_2 mixture at 673 K for 1 h. After sulfidation, the samples were stored and manipulated under isooctane to avoid reoxidation of the sulfides by atmospheric air. The hydrocarbon was eliminated under vacuum in the pre-treatment chamber of the XPS instrument.

2.3. Catalytic measurements

2.3.1. Cumene hydrocracking

Catalytic activity in cumene hydrocracking was measured in a conventional continuous flow microreactor system (ca. 100 mg catalyst weight) at 623 K and 2.8 MPa pressure, under a 300 $cm^3\ min^{-1}$ (STP) flow of hydrogen and a 10.6 $cm^3\ h^{-1}$ liquid feed flow-rate. The feed was composed of 16% (v/v) cumene and 0.66% (v/v) CS_2 dissolved in *n*-hexane. Before each run, the catalysts were sulfided under the same conditions described for the XPS experiments. Specific reaction rates in $\mu mol\ g^{-1}\ min^{-1}$ were obtained from conversion values assuming first order reaction kinetics with respect to cumene.

2.3.2. Thiophene HDS

Thiophene HDS was carried-out using ca. 200 mg catalyst weight, in the same reactor system as cumene HCC, in the 523–573 K temperature range and 2.8 MPa pressure, under a 300 $cm^3\ min^{-1}$ (STP) flow of hydrogen and 10.8 $cm^3\ h^{-1}$ liquid feed flow-rate. The feed was composed of 2.65 wt.% thiophene (1 wt.% S) dissolved in *n*-hexane. The catalysts were sulfided under the same conditions described above. Specific reaction rates in $\mu mol\ g^{-1}\ min^{-1}$ were obtained from conversion values assuming first order reaction kinetics with respect to thiophene.

3. Results and discussion

3.1. XPS characterization

Catalyst compositions and surface areas are shown in Table 1. The last column in Table 1 shows the surface areas expressed per mass of support. It is clear that impregnation of the AL and of the NB support does not cause a significant decrease in surface area as compared to the original area of the support. In contrast, with the NBP support the loss of surface area, especially with the molybdenum-containing catalysts, was rather large.

Table 1
Compositions and surface areas of the catalysts

Sample	MoO_3[a]	NiO[a] (wt.%)	P[a] (wt.%)	Ni/Mo[b] (wt.%)	S.A.[c] ($m^2\ g^{-1}$)	S.A.[d] ($m^2\ g^{-1}$)
NB[e]	–	–	–	–	65	–
NB-M[e]	8.2	–	–	–	54	59
NB-N2[e]	–	3.4	–	–	70	73
NB-N3[e]	–	5.0	–	–	65	68
NB-NM1[e]	8.2	1.5	–	0.4	52	58
NB-NM2[e]	8.1	3.0	–	0.7	47	53
NB-NM3[e]	7.9	4.5	–	1.1	47	54
NBP	–	–	7.2	–	70	–
NBP-M	8.3	–	6.6	–	34	37
NBP-N2	–	3.5	7.1	–	51	53
NBP-N3	–	4.9	6.9	–	45	47
NBP-NM1	8.2	1.4	6.4	0.3	25	28
NBP-NM2	8.0	3.0	6.4	0.7	26	29
NBP-NM3	7.8	4.3	6.3	1.1	21	24
AL[e]	–	–	–	–	247	–
AL-M[e]	18.4	–	–	–	227	278
AL-N1[e]	–	4.0	–	–	230	240
AL-N2[e]	–	7.8	–	–	231	251
AL-N3[e]	–	11.3	–	–	224	253
AL-NM1[e]	18.3	3.3	–	0.4	200	255
AL-NM2[e]	17.7	6.2	–	0.7	197	258
AL-NM3	16.9	9.3	–	1.1	182	247

[a] Chemical composition determined by X-ray fluorescence.
[b] Atomic ratio.
[c] BET surface area.
[d] BET surface area per mass of support.
[e] Ref. [20].

We have shown before that, during sulfidation of niobia-supported Mo or Ni catalysts, a surface niobium sulfide is formed in amounts depending on the nature and loading of the supported elements [19]. We also showed that this occurs to a much smaller extent with the catalysts additivated with phosphorus. The amount of sulfur associated with the surface niobium sulfide, $[S_{Nb}]_{XPS}$, may be estimated by subtracting the amount of sulfur required to completely sulfide the nickel and molybdenum in the catalysts from the total sulfur atomic concentration measured by XPS $[S_{tot}]_{XPS}$, according to the following formula:

$$[S_{Nb}]_{XPS} = [S_{tot}]_{XPS} - 2[Mo^{4+}]_{XPS} - (3/2)[Ni]_{XPS}$$

where it is assumed that only the molybdenum in the 4+ oxidation state is sulfided to produce MoS_2 and that the sulfided nickel has stoichiometry Ni_3S_2.

Fig. 1 shows that the linear correlation between the amount of niobium-associated sulfur and the amount of niobium reduced to the 4+ state, found before with the niobia-supported Ni or Mo catalysts [19], is maintained when the bimetallic Ni–Mo catalysts are included. The slope of the straight line is very close to the one obtained before, namely 2.1, indicating that a sulfide with stoichiometry close to NbS_2 is obtained. The

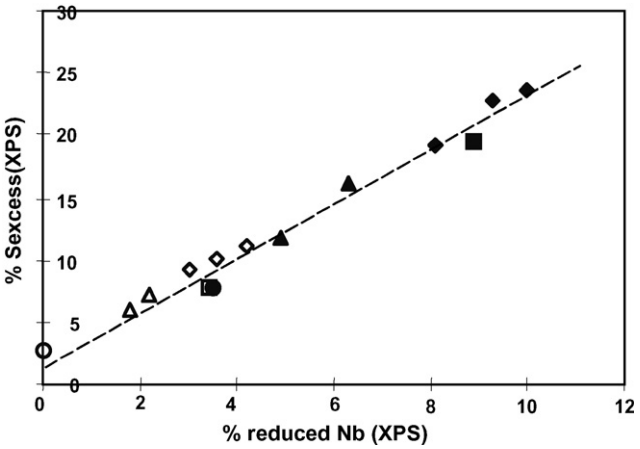

Fig. 1. Correlation between XPS sulfur atomic concentration in excess of the necessary to sulfide the Ni and Mo in the catalysts vs. XPS reduced niobium atomic fraction. Circles, supports; squares, Mo catalysts; triangles, Ni catalysts; diamonds, Ni–Mo catalysts; filled symbols, NB support; open symbols, NBP support.

Table 2
Quantitative XPS analysis for molybdenum

Catalyst	Mo/Nb(+P)[a]		Mo/Al[a]	
	Oxide[b]	Sulfided	Oxide[b]	Sulfided
NB-M	0.12	0.18	–	–
NB-NM1	0.14	0.18	–	–
NB-NM2	0.13	0.19	–	–
NB-NM3	0.06	0.19	–	–
NBP-M	0.13	0.14	–	–
NBP-NM1	0.15	0.16	–	–
NBP-NM2	0.12	0.17	–	–
NBP-NM3	0.14	0.19	–	–
AL-M	–	–	0.085	0.085
AL-NM1	–	–	0.10	0.089
AL-NM2	–	–	0.084	0.092
AL-NM3	–	–	0.090	0.093

[a] XPS atomic ratios. In the case of the NBP support the ratios are taken with respect to Nb + P.
[b] Ref. [20].

conclusion that phosphorus inhibits the reduction sulfidation of niobium is also confirmed. According to Jehng et al. [21], modification of niobia with phosphate leads to the formation of a phosphate surface overlayer that presumably protects the niobia surface against reduction.

It is seen that, within each series (NB and NBP), the degree of reduction/sulfidation of the niobium follows the order Ni–Mo > Mo > Ni > support, with exception of the Ni–Mo catalysts with the lowest nickel content, where formation of the niobium sulfide occurs to an extent similar to the one observed with the molybdenum catalysts.

In Fig. 1, the degree of niobium reduction/sulfidation follows the same order as the nickel content, both in the NB and in the NBP series and when both Ni and Ni–Mo catalysts are considered. The extent of niobium reduction/sulfidation therefore increases with the hydrogenating power of the supported sulfides, which suggests that hydrogen spillover plays an important role in the process. It is well known that niobium oxide is partially reducible when exposed to hydrogen at high pressure and the reduction is accelerated by the presence of zero-valent metals on its surface [22,23]. More recently Afanasiev et al. have shown that sulfidation of a mixed Mo–Nb oxide to produce a mixed Mo–Nb sulfide is much easier than that of Nb_2O_5 [24].

Table 2 shows the results of the quantitative XPS analysis for molybdenum in the catalysts, both in the oxide and in the sulfided form, in terms of Mo/Nb and Mo/Al atomic ratios. In the case of the NBP series, the atomic ratio is taken with respect to niobium plus phosphorus. The XPS results for the oxide form of the catalysts supported on AL and NB have been discussed in our previous publication [20]. It should only be added here that the values obtained for molybdenum with the catalysts supported on NBP were very similar to the ones obtained with the NB series of catalysts, indicating that the molybdenum dispersion and distribution are similar in both cases. In this paper we focus on the changes in atomic XPS ratios that accompany sulfidation.

With the catalysts supported on AL, the XPS Mo/Al ratios of the sulfided samples are very close to those of the oxidic form of the catalysts. Those, on their turn, are close to the bulk ratios determined by X-ray fluorescence. According to the model developed by Kerkhof and Moulijn for quantitative interpretation of XPS results [25], for high surface area supports (photolectron escape-depth similar the thickness of the walls of the support), a monolayer dispersion of the supported phase leads to compositions determined by XPS close to the bulk ones. This means that the molybdenum dispersion remained close to the monolayer value after sulfidation of the alumina-supported Mo and Ni–Mo catalysts.

In contrast there was a large increase in the XPS Mo/(Nb + P) ratio upon sulfidation with the catalysts supported on NBP. This effect was even more pronounced with the Mo/Nb ratios in the NB series of catalysts. Our results on the characterization of the oxide form of the catalysts [20] suggested that a strong interaction between molybdenum and niobium oxides exists, possibly with formation of a mixed Mo–Nb oxide and consequent migration of part of the molybdenum to subsurface layers of the support. Destruction of this interaction species upon sulfidation may have increased the molybdenum surface concentration. With the NBP catalysts, the increase in surface molybdenum concentration during sulfidation was only pronounced for the catalysts with the largest nickel contents, NBP-NM2 and NBP-NM3. This is consistent with the fact that, of the catalysts supported on NBP, those are the ones where reduction/sulfidation of the niobium is largest and therefore the destruction of the Mo–Nb interaction species must have occurred to the largest extent.

Table 3 shows molybdenum 3d binding energies obtained by deconvolution of the peaks in the region 220–240 eV of the high resolution XPS spectra of the sulfided catalysts. Binding energies for the $3d_{3/2,5/2}$ doublet of Mo^{4+} (ca. 229 and 232 eV, respectively [26,27]) were smaller on the NB and NBP-supported catalysts by 0.4–0.5 eV than on the alumina-supported ones, which may be attributed to different degrees of

Table 3
XPS binding energies (in eV units) and Mo^{4+}/Mo^{5+} ratios

Catalyst	Mo^{4+} (1)		Mo^{5+}		Mo^{4+}/Mo^{5+}
	$3d_{5/2}$	$3d_{3/2}$	$3d_{5/2}$	$3d_{3/2}$	
NB-M	228.8	232.0	230.6	233.8	3.3
NB-NM1	228.6	231.8	230.2	233.4	2.8
NB-NM2	228.8	232.0	230.3	233.5	2.1
NB-NM3	228.6	231.8	230.3	233.5	3.0
NBP-M	228.8	232.0	230.2	233.4	3.4
NBP-NM1	228.6	231.8	230.1	233.3	3.0
NBP-NM2	228.7	231.9	230.4	233.6	3.2
NBP-NM3	228.7	231.9	230.5	233.7	3.2
AL-M	229.0	232.2	230.8	234.0	12.0
AL-NM1	229.2	232.4	231.8	235.0	7.6
AL-NM2	229.2	232.4	231.6	234.8	6.9
AL-NM3	229.2	232.3	231.0	234.2	6.1

interaction with the supports or perhaps to the contribution of a mixed Mo–Nb sulfide. Within each series of catalysts, no significant differences in binding energies were observed.

With the Mo^{5+} doublet (ca. 231 and 235 eV [25,26]), the difference between the alumina-supported and the niobia-supported catalysts was in excess of 1 eV. These incompletely reduced Mo species are most likely in strong interaction with the support [28], and therefore have niobium or aluminum ions in their close vicinity. Because of the smaller cation electronegativity of Al^{3+} as compared to Nb^{5+} (10.5 and 17.6, respectively, using Tanaka and Ozaki's method [29]), the Mo–O bond of molybdenum ions close to Al^{3+} is more polarized, therefore the effective charge on Mo^{5+} is larger and consequently also the XPS binding energy.

Table 3 also shows results for the Mo^{4+}/Mo^{5+} ratio. As found before with the monometallic Mo catalysts [19], the reducibility of molybdenum is considerably smaller with the bimetallic catalysts supported on NB and NBP, possibly because of the formation of the mixed Mo–Nb oxide. Our previous TPR results with NB-M and AL-M catalysts confirm this interpretation [20]. It is also clear from Table 3 that this effect is slightly smaller with the catalysts supported on NBP than with those supported on NB, possibly because the presence of phosphorus somewhat inhibits formation of the Mo–Nb mixed-oxide species.

Results for the quantitative XPS analysis for nickel are shown in Table 4, both for the oxide and the sulfided forms of the catalysts, in terms of Ni/Nb and Ni/Al atomic ratios. In the case of the NBP series, the atomic ratio is taken with respect to niobium plus phosphorus. As in the case of molybdenum, results for the oxide form of the catalysts were discussed in our previous publication and we focus here on the modifications of atomic ratios that accompany catalyst sulfidation. It should only be added here that the results for the NBP series of catalysts were generally similar to the ones obtained with the NB series.

The results in Table 4 clearly show that there is a large decrease in the apparent surface nickel concentration upon sulfidation of the alumina-supported monometallic catalysts. This may be attributed to sintering of the supported nickel to form relatively large nickel sulfide particles. With the

Table 4
Quantitative XPS analysis for nickel

Catalyst	Ni/Nb(+P)[a]		Ni/Al[a]	
	Oxide[b]	Sulfided	Oxide[b]	Sulfided
NB-N2	0.040	0.054	–	–
NB-N3	0.064	0.087	–	–
NB-NM1	nd[c]	0.056	–	–
NB-NM2	0.089	0.094	–	–
NB-NM3	0.20	0.15	–	–
NBP-N2	0.058	0.057	–	–
NBP-N3	0.082	0.083	–	–
NBP-NM1	nd[c]	0.058	–	–
NBP-NM2	0.079	0.090	–	–
NBP-NM3	0.12	0.12	–	–
AL-N1	–	–	0.036	0.019
AL-N2	–	–	0.062	0.026
AL-N3	–	–	0.083	0.044
AL-NM1	–	–	0.028	0.025
AL-NM2	–	–	0.050	0.040
AL-NM3	–	–	0.076	0.051

[a] XPS atomic ratios. In the case of the NBP support, the ratios are taken with respect to Nb + P.
[b] Ref. [20].
[c] Not detected.

bimetallic catalysts, the loss of nickel dispersion is much smaller, but increases with nickel content. It has been proposed that a mixed Ni–Mo sulfide is formed upon sulfidation of alumina-supported Ni–Mo catalysts (NiMoS phase [30]), where nickel atoms decorate the edges of hexagonal molybdenum IV sulfide crystallites. This should prevent the growth of nickel sulfide particles, but only to the extent to which the edges of molybdenum sulfide crystallites are able to accommodate the nickel atoms, which may explain the observed effects. With the niobia-supported catalysts the effect of sulfidation on nickel dispersion is modest. This suggests that interaction with the niobia supports prevents the sintering of nickel during sulfidation and also that a Ni–Mo interaction species is formed to a much smaller extent in this case, since little effect of molybdenum addition is found.

3.2. Cumene hydrocracking

Cumene hydrocracking is a well-known probe for the presence of Brønsted acidic sites on catalytic surfaces [31]. Results for catalytic activity in this reaction have been presented before for the monometallic catalysts [19]. A good linear correlation was found between the specific activity (catalyst mass basis) in cumene hydrocracking and the amount of sulfided niobium in the catalysts, suggesting that the niobium sulfide is the main species responsible for the reaction. In this case, however, a correlation involving the specific activity is not the most appropriate one, since there were large differences in surface area between the NB and the NBP series of catalysts. Fig. 2 shows the results for the correlation between the intrinsic activity (catalyst area basis) and the amount of reduced niobium. It is worth noticing that intrinsic rates were calculated using the surface areas of the unsulfided catalysts. The surface

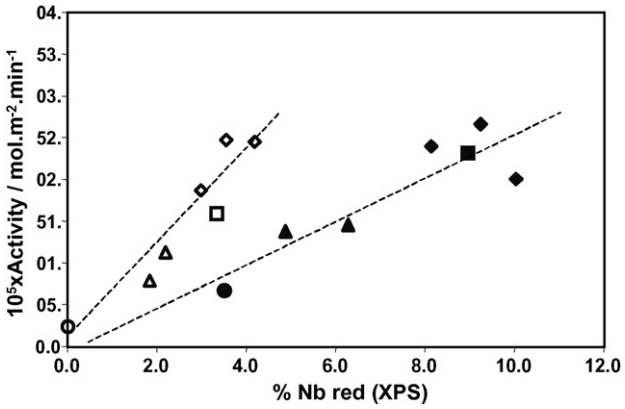

Fig. 2. Intrinsic activity in cumene hydrocracking at 623 K and 2.8 MPa vs. XPS reduced niobium atom fraction (normalized with respect to the surface areas of the unsulfided catalysts). Circles, supports; squares, Mo catalysts; triangles, Ni catalysts; diamonds, Ni–Mo catalysts; filled symbols, NB support; open symbols, NBP support.

areas of some of the sulfided samples were measured and did not differ by more than 10% from those of the unsulfided samples. In this graph, the NB- and the NBP-supported catalysts fall on different groups, but in each case a reasonable linear correlation is found.

Phosphate is seen to promote the acidic activity of the sulfided niobium. The larger intrinsic activity of the NBP-supported catalysts cannot be attributed to the action of phosphate itself, since the activity of the sulfided support is much smaller than those of all of the sulfided catalysts, but rather to a combined effect of the presence of phosphate and niobium reduction/sulfidation.

3.3. Thiophene HDS

Thiophene HDS was studied at 2.7 MPa total pressure and in the 523–573 temperature range. Table 5 shows the results for intrinsic reaction rates at 543 K, normalized with respect to the surface areas of the unsulfided samples. It is first noticed that the sulfided NB support has a measurable activity in this reaction, which is consistent with the fact the some sulfidation of this material occurred, as indicated by the XPS measurements. In line with this observation, the sulfided NBP support, in which formation of niobium sulfide was not observed, has no activity in this reaction.

For the same metal loading (on a per surface area basis) the monometallic molybdenum catalysts supported on NB and NBP have a smaller activity than the alumina-supported one. This may be related to the formation of a mixed Mo–Nb sulfide, which according to Afanasiev et al. [24], has intermediate activity between the monometallic sulfides.

On the other hand, the NB and NBP-supported monometallic nickel catalysts have activities larger by an order of magnitude as compared to the alumina-supported one. This is probably the combined effect of a higher dispersion of the niobia-supported nickel sulfide, as revealed by the XPS measurements, and of the contribution of the sulfided supports themselves.

With the alumina-supported bimetallic catalysts the well known strong synergetic effect between molybdenum and nickel is observed. This occurs, if at all, to a much smaller extent with the materials supported on NB and NBP. The synergetic effect between molybdenum and nickel is generally attributed to the formation of the NiMoS phase mentioned above [30,32]. Apparently this phase is not formed with the niobia-supported catalysts, which is consistent with the fact that molybdenum and nickel interact preferentially with the niobia support rather than with each other, as shown by the characterization of the oxide form of the catalysts [20] and the XPS results presented here.

Good linear Arrhenius plots (ln r versus $1/T$) were obtained for all catalysts in the 523–573 K temperature range. The apparent activation energies derived from these plots are shown in Table 6. Significant differences are observed between the alumina-supported monometallic and bimetallic catalysts, indicating that the active species in the bimetallic catalysts (NiMoS phase) is distinct from the active species in the monometallic ones.

The apparent activation energy for the sulfided niobia support is larger than the one obtained with the alumina-supported molybdenum catalyst. With the NB- and NBP-supported monometallic catalysts, apparent activation energies were intermediate between those of the alumina-supported ones and the sulfided niobia support. This means that both the sulfided niobium and the supported sulfides contribute to the

Table 5
Activities in thiophene HDS at 2.7 MPa and 543 K[a]

	Mo[b]	Ni[b]	AL[c]	NB[d]	NBP[e]
Support	0	0	0	3.2	0
Support-M	4.6	0	7.2	5.9	5.2
Support-N2	0	3.7	0.9	7.6	6.5
Support-N3	0	5.5	0.8	9.8	9.5
Support-NM1	4.6	1.6	147	8.0	17.0
Support-NM2	4.6	3.7	149	10.8	19.8
Support-NM3	4.6	5.5	132	13.3	26.6

[a] Expressed in μmol m^{-2} h^{-1} based on surface area of the oxide form.
[b] Metal loadings in atoms nm^{-2} based on surface area of the support.
[c] Alumina-supported catalysts.
[d] Niobia-supported catalysts.
[e] Phosphated niobia-supported catalysts.

Table 6
Activation energies for thiophene HDS at 2.7 MPa pressure[a]

	Mo[b]	Ni[b]	AL[c]	NB[d]	NBP[e]
Support	0	0	–	120	–
Support-M	4.6	0	80	109	103
Support-N2	0	3.7	71	114	105
Support-N3	0	5.5	98	110	108
Support-NM1	4.6	1.6	118	110	110
Support-NM2	4.6	3.7	117	105	104
Support-NM3	4.6	5.5	113	106	116

[a] Obtained in the 523–573 K temperature range and expressed in kJ mol^{-1}.
[b] Metal loadings in atoms nm^{-2} based on surface area of the support.
[c] Alumina-supported catalysts.
[d] Niobia-supported catalysts.
[e] Phosphated niobia-supported catalysts.

catalytic activity. The values obtained with the NBP series of monometallic catalysts were systematically lower than those corresponding to the NB series and therefore closer to those obtained with the alumina-supported catalysts. This is consistent with the fact that the degree of niobium sulfidation is smaller with the NBP-supported catalysts and therefore the contribution of the niobium sulfide is correspondingly smaller.

The apparent activation energies for the NB- and NBP-supported bimetallic catalysts were slightly but systematically (with the only exception of catalyst NBP-NM3) lower than the ones obtained with the alumina-supported catalysts and there was a much smaller change from the monometallic to the bimetallic catalysts than in the alumina case. This is consistent with the fact that a NiMoS phase is not formed to an appreciable extent in the niobia-supported catalysts.

4. Conclusions

The results presented here confirm that, also with bimetallic niobia-supported Ni–Mo catalysts, a surface niobium sulfide with stoichiometry close to NbS_2 is formed upon sulfidation with a H_2S/H_2 mixture at 673 K. The degree of niobium sulfidation increases in the order $Nb_2O_5 < Ni/Nb_2O_5 < Mo/Nb_2O_5 < NiMo/Nb_2O_5$ and is strongly inhibited by the presence of phosphorus on the support.

This niobium sulfide is responsible for the activity of the niobia-supported catalysts in the cumene hydrocracking reaction. The intrinsic activity in this reaction was larger with the catalysts supported on phosphate-additivated niobia than with those supported on pure niobia.

From the XPS results, the dispersion of nickel sulfide is larger on the niobia supports than on alumina.

The reducibility of molybdenum is smaller with the niobia-supported catalysts than with the alumina-supported ones due to existence of a strong molybdena–niobia interaction in the oxide form of the catalysts.

The sulfided niobia support has a measurable activity in thiophene HDS, corresponding to about half of the intrinsic activity measured with alumina-supported molybdenum. Despite that fact, the activity of niobia-supported molybdenum sulfide is smaller than that of the alumina-supported catalyst, partly due to the smaller degree of reduction of the molybdenum when supported on niobia, but also possibly due to the formation of a mixed Nb–Mo sulfide with thiophene HDS activity intermediate between those of the monometallic sulfides [24].

On the other hand, for comparable nickel loadings (on a support surface area basis), nickel sulfide has a much higher activity when supported on niobia than when supported on alumina. This is the combined effect of a higher dispersion of the nickel sulfide and the contribution of the sulfided niobia support to the activity.

In contrast with the alumina case, there is little synergetic effect between molybdenum and nickel with the niobia-supported catalysts in the thiophene HDS reaction. Also in contrast with the alumina case, activation energies for thiophene HDS changed little from the monometallic to the bimetallic catalysts. These facts indicate that a NiMoS phase is formed to a very limited extent with the niobia-supported catalysts, if at all.

Overall, niobia-supported Ni–Mo catalysts, and therefore possibly other catalyst compositions containing the Ni–Mo–Nb combination, may be useful when an acidic function is desired, such as in hydrocracking, but their HDS activity is limited.

Acknowledgements

This work is dedicated to the memory of Prof. Paul Grange, in whose laboratory at the University of Louvain, Belgium, the XPS spectra were obtained. We thank PETROBRAS R&D center, for technical and financial support to this project.

References

[1] American Petroleum Institute and National Petroleum Refiners Association, 1996 American Petroleum Institute/National Petroleum Refiners Association Survey of Refining Operations and Product Quality, API Publishing Services, Washington DC, 1997
[2] European Automobile Manufacturers Association, Alliance of Automobile Manufacturers, Engine Manufacturers Association and Japan Automobile Manufacturers Association, World-wide Fuel Charter, 2000. See also: http://www.engine-manufacturers.org/about/Final WWFC 4 00.pdf.
[3] R.B. Quincy, M. Houalla, A. Proctor, D.M. Hercules, J. Phys. Chem. 93 (1989) 5882.
[4] J. Ramirez, S. Fuentes, G. Diaz, M. Vrinat, M. Breysse, M. Lacroix, Appl. Catal. 52 (1989) 211.
[5] J.C. Duchet, M.J. Tilliette, D. Cornet, L. Vivier, G. Perot, L. Bekakra, C. Moreau, G. Szabo, Catal. Today 10 (1991) 579.
[6] D. Hamon, M. Vrinat, M. Breysse, B. Durand, F. Beauchesne, T. Descourieres, Bull. Soc. Chim. Belg. 100 (1991) 933.
[7] A. Nishijima, H. Shimada, T. Sato, Y. Yoshimura, J. Hiraishi, Polyhedron 5 (1986) 243.
[8] M. Breysse, J.L. Portefaix, M. Vrinat, Catal. Today 10 (1991) 489.
[9] T. Iizuka, K. Ogasawara, K. Tanabe, Bull. Chem. Soc. Jpn. 56 (1983) 2927.
[10] M. Danot, J.C. Afonso, M. Breysse, T. Courieres, Catal. Today 10 (1991) 629.
[11] A. Florentino, P. Cartraud, P. Magnoux, M. Guisnet, Appl. Catal. A 89 (1992) 143.
[12] N. Allali, A.M. Marie, M. Danot, C. Geantet, M. Breysse, J. Catal. 156 (1995) 279.
[13] J.C. Afonso, PhD Thesis, Université Claude Bernard, Lyon I, 1990.
[14] M. Vrinat, C. Guillard, M. Lacroix, M. Breysse, M. Kurdi, M. Danot, Bull. Soc. Chim. Belg. 96 (1987) 1017.
[15] C. Geantet, J. Afonso, M. Breysse, N. Allali, M. Danot, Catal. Today 28 (1996) 23.
[16] S.J.V. Machado, M. Schmal, A.C. Faro Jr., in: Proceedings of the Fifth Brazilian Seminar on Catalysis, Guarujá, (1989), p. 667.
[17] J.G. Weissman, Catal. Today 28 (1996) 159.
[18] A.C.B. dos Santos, W.B. Kover, A.C. Faro Jr., Appl. Catal. A: Gen. 153 (1997) 83.
[19] A.C.B. dos Santos, P. Grange, A.C. Faro Jr., Appl. Catal. A: Gen. 178 (1999) 29.
[20] A.C. Faro Jr., P. Grange, A.C.B. dos Santos, Phys. Chem. Chem. Phys. 4 (2002) 3997.
[21] J.M. Jehng, A.M. Turek, I.E. Wachs, Appl. Catal. A: Gen. 83 (1992) 179.
[22] S.J. Tauster, S.C. Fung, J. Catal. 55 (1978) 29.
[23] G. Sankar, S. Vasudevan, C.N.R. Rao, J. Phys. Chem. 92 (1988) 1878.

[24] P. Afanasiev, L. Fischer, F. Beauchesne, M. Danot, V. Gaborit, M. Breysse, Catal. Lett. 64 (2000) 59.
[25] F.P.J.M. Kerkhof, J.A. Moulijn, J. Phys. Chem. 83 (1979) 1612.
[26] J.R. Brown, M. Ternan, Ind. Eng. Chem. Prod. Res. Dev. 23 (1984) 557.
[27] L.E. Makovsky, J.M. Stencel, F.R. Brown, R.E. Tischer, S.S. Pollack, J. Catal. 89 (1984) 334.
[28] Y. Okamoto, A. Maezawa, T. Imanaka, J. Catal. 120 (1989) 29.
[29] K. Tanaka, A. Ozaki, J. Catal. 8 (1967) 2.
[30] N.-Y. Topsøe, H. Topsøe, J. Catal. 84 (1983) 386.
[31] A. Corma, B.W. Wojciechowski, Catal. Rev. Sci. Eng. 24 (1982) 1.
[32] H. Topsøe, B.S. Clausen, F.E. Massoth, in: J.R. Anderson, M. Boudart (Eds.), Catalysis—Science and Technology, vol. 11, Springer, 1996.